

Photoemission experiments on YbInCu_4 : Surface effects and temperature dependence

F. Reinert, R. Claessen, G. Nicolay, D. Ehm, and S. Hüfner
Fachrichtung Experimentalphysik, Universität des Saarlandes, 66041 Saarbrücken, Germany

W. P. Ellis
Los Alamos National Laboratory, Los Alamos, New Mexico 87545

G.-H. Gweon and J. W. Allen
Randall Laboratory, University of Michigan, Ann Arbor, Michigan 48109-1120

B. Kindler and W. Assmus
Physikalisches Institut, Universität Frankfurt, 60054 Frankfurt, Germany
 (Received 20 November 1997; revised manuscript received 25 February 1998)

We present temperature-dependent photoemission (PES) measurements on single-crystalline YbInCu_4 , a stoichiometric material that shows an isostructural first-order valence transition at $T_a \approx 60$ K. The results of the analysis of the PES data show peculiar differences to other, bulk-sensitive measurements: (a) a lack of the sharp first-order valence transition and (b) the Yb valence — determined directly from the $4f$ intensity ratio — lies substantially below x-ray absorption (XAS) results over the whole investigated temperature range. We discuss these discrepancies with particular attention to surface effects and conclude that the PES results are due to a distorted near-surface region which differs in its physical properties significantly from the volume material. [S0163-1829(98)08843-2]

I. INTRODUCTION

The valence-fluctuating compound YbInCu_4 shows a peculiar iso-structural first-order phase transition at ambient pressure with an abrupt increase in the lattice constant of about 0.13%,^{1,2} reminiscent of the $\alpha \rightarrow \gamma$ phase transition in metallic Ce. Depending on the exact stoichiometry of the sample the transition temperature T_a varies from approximately 40 K to 70 K.¹⁻⁴ Going below the transition temperature the electrical resistivity drops by one order of magnitude, while the magnetic susceptibility changes from a strict Curie-Weiss behavior ($\mu_{\text{eff}} = 4.64 \mu_B$) to an essentially temperature-independent Pauli-paramagnetism. In addition, the elastic constants show a steplike anomaly at the transition temperature. The experimental width of the transition lies typically below 10 K. By a variety of techniques¹⁻³ it has been established that in going below the transition temperature the valence ν of the Yb ions decreases from a value close to Yb^{3+} to a more mixed-valent state by about 0.1.

First photoemission spectroscopy (PES) measurements at 10, 80, and 293 K on polycrystalline samples showed a temperature variation in the intensity ratio of the Yb $4f^{13}$ (divalent) to Yb $4f^{12}$ (trivalent) final-states.⁵ This ratio can be used to determine the Yb valence from the PES Yb $4f$ spectra, yielding a valence change from $\nu = 2.63$ at 293 K to $\nu = 2.38$ at both 10 and 80 K. A more recent study of the temperature dependence of the Yb $4f^{13}$ states by high-resolution PES (Ref. 6) confirmed a temperature dependence of the $4f^{13}$ intensity and associated it with the ‘‘Kondo scenario’’ of the single impurity Anderson model (SIAM), which relates the valence change to a thermal excitation of magnetic triplet states from a singlet ground state. This concept describes successfully the thermal properties of various

rare-earth systems⁷ and was previously applied to the analysis of photoemission data of other Yb compounds like YbAl_3 (Ref. 8) or YbAgCu_4 .^{9,10}

However, the applicability of the SIAM to the analysis of photoemission data of mixed valent rare-earth compounds (especially Ce and Yb systems) has recently been the subject of a controversy, in particular with respect to PES results on YbAl_3 .^{8,11-13} It has been discussed whether the apparent temperature dependence of the divalent spectral weight is due to the temperature dependence of the Yb valence, described by the SIAM, or whether it can be explained entirely by conventional effects, like surface and phonon contributions, which are known from core-level spectra of simple metals.^{14,15}

The most common spectroscopic methods to determine the Yb valence of an intermediate valent system are x-ray absorption (XAS) at the L_{III} edge and PES on the $4f$ states. With photon energies near 9 keV XAS probes the bulk of the sample whereas the mean free path length of the photoelectrons makes the PES an extremely surface sensitive technique, in which the sampling depth is confined (dependent on the kinetic energy of the photoelectrons) to the first few atomic layers. It was already noted that for a variety of intermediate-valent Yb compounds the Yb valence derived from the $4f$ PES remains significantly below that obtained from the L_{III} XAS edges, which led to the speculation¹⁶ that in these materials the surface region probed by PES could be different from the volume.

In YbInCu_4 the first-order valence transition at T_a , being well studied by volume-sensitive methods, provides an additional chance to test the extent to which surface-sensitive PES measurements are in accordance with the properties of the bulk material.

Here we present temperature-dependent PES measurements on single-crystalline YbInCu₄ samples. The analysis of the data shows that the PES results are indeed substantially influenced by surface effects. The intrinsic temperature dependence of the Yb *4f* spectral weight shows a significant variation of the Yb valence over the investigated temperature range from 20 to 200 K, but it is gradual and shows no indication of the sharp transition at $T_a \approx 60$ K. In addition, the PES valences of the sampled Yb ions are over the whole temperature range found to remain consistently below that obtained by XAS and other bulk sensitive methods.^{1,17} These discrepancies point towards the existence of a subsurface zone, different from the bulk.

II. SAMPLES AND INSTRUMENTATION

The single crystals (C15b-type Laves-phase structure) were prepared from purified metallic Yb, In, and Cu using the Bridgman method. Stoichiometric amounts of the three ingredients were placed in an evacuated tantalum tube. Due to the high vapor pressure of Yb metal at the melting temperature of about 1000 °C, both ends of the tube were sealed by arc welding under Ar atmosphere. The mixture in the crucible was homogenized by heating to 1100 °C for about half an hour. In the Bridgman procedure, the growth of the crystal is controlled by moving the crucible slowly (with a velocity of 2 mm/h) along a temperature gradient to lower temperatures. The duration of the process amounted to 30–35 h.

The crystals were characterized by Laue diffraction and energy dispersive x-ray (EDX) analysis. No bulk impurities could be detected. Depending on exact stoichiometry and slight disorder the transition temperature T_a can vary from about 40 to 70 K, nonetheless maintaining the first-order character of the transition.^{1,4,18–20} For the samples presented here T_a is approximately 65 K. The width of the transition is smaller than 10 K, as determined from, e.g., the magnetic susceptibility and the elastic constants. A detailed description of the crystal growth and characterization can be found in Refs. 2 and 21.

For the PES measurements the original crystals have been cut to smaller pieces ($\approx 3 \times 2 \times 2$ mm³). These crystals were attached to an aluminum sample holder, oriented by Laue diffraction, electrically contacted, and finally equipped with a cleavage post. Though the *in situ* cleavage of the crystals did not expose well-defined crystal planes but rather fractured surfaces, their PES spectra were found to reflect an electronically homogeneous and atomically clean surface. As an alternative method of surface preparation the samples could be scraped *in situ* by a diamond file.

The PES data were obtained at the undulator beam lines U2-FSGM at the BESSY storage ring in Berlin and 5-3 at the Stanford Synchrotron Radiation Laboratory (SSRL). The photoemission spectrometers were a VG-ESCALAB instrument and a VSW angular-resolved photoelectron spectrometer, respectively. The overall energy resolutions were 39 meV at a photon-energy of $h\nu = 22.4$ eV and 80 meV at 43 eV. By use of a He cryostat the sample temperature could be varied from below 20 K up to room temperature (RT). The base pressure was better than 5×10^{-11} mbar in both setups.

All spectra were normalized to the intensity *above* the

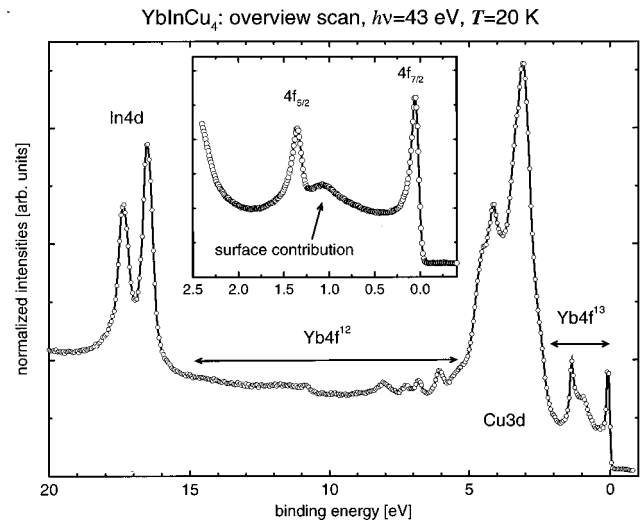


FIG. 1. Valence-band (VB) spectra of a freshly cleaved YbInCu₄ surface, taken at $h\nu = 43$ eV and $T = 20$ K. The inset shows in more detail the range of the Yb $4f^{13}$ “bulk” and surface final-state structures.

Fermi energy, which results from second-order light excitation and can be used as a measure of the incident photon flux. Application of this normalization procedure results in an excellent match of the In *4d*, Cu *3d*, and conduction-band intensities of spectra that were measured at different times after storage ring injection at the same photon energy. It was also tried to measure the angular dispersion in several directions perpendicular to the surface normal [(100) and (110)], but neither energy dispersion (within an experimental uncertainty of 5 meV) nor pronounced intensity variation of the Yb $4f_{7/2}^{13}$ peak could be detected. It remains undecided whether this reflects a high degree of *4f* localization or whether a possible small *4f* dispersion is obscured by imperfections of the cleaved surface.

III. EXPERIMENTAL RESULTS

A. Valence-band spectra

Figure 1 shows a wide valence-band scan of a freshly cleaved YbInCu₄ single-crystal surface, measured at $T = 20$ K with a photon energy $h\nu = 43$ eV. The most prominent structures are the In *4d* spin-orbit doublet at ≈ 17 eV and the Cu *3d* band ranging from 5 to 2.5 eV. Due to the strong on-site correlation of the Yb *4f* electrons the corresponding photoemission final states appear in two clearly separated energy ranges: a widely spread multiplet between binding energies $E_B = 5$ and 15 eV, and a narrow doublet near the Fermi energy ($E_B = 0$) with a spin-orbit splitting of 1.3 eV.²² These two Yb *4f* features originate from the $4f^{12}$ (trivalent) and $4f^{13}$ (divalent) PE final states, respectively. Their intensity ratio is determined by the number of *4f* electrons in the initial ground state, and is therefore related to the *4f* hole occupancy n_h and to the Yb valence $v = 2 + n_h$. In addition to the Yb $4f^{13}$ bulk states there exists a broader surface contribution, which originates from a valence change of the outermost atoms to divalent Yb²⁺, accompanied by a surface core-level shift (SCLS) of the $4f_{7/2}^{13}$ component of ≈ 1.1 eV to higher binding energies^{23,24} (see inset of Fig. 1). Its 5/2 spin-orbit partner at ≈ 2.1 eV is obscured by the tail

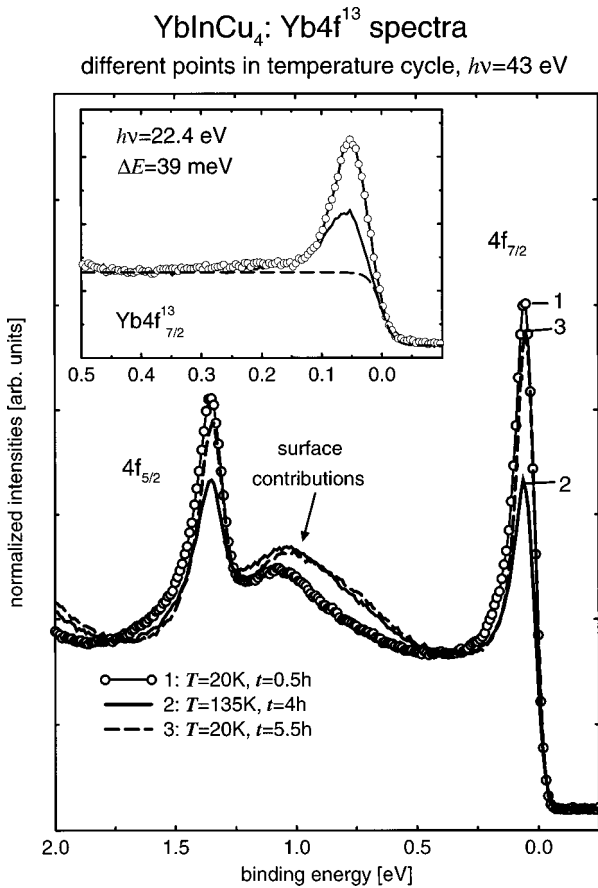


FIG. 2. Comparison of three Yb $4f^{13}$ spectra at $h\nu=43$ eV, taken at 20 K (1), 135 K (2), and again 20 K (3). The numbers are identical to the points 1, 2, and 3 in the graph of Fig. 3. The inset shows high-resolution ($\Delta E=39$ meV) spectra taken with $h\nu=22.4$ eV. The dashed line represents the assumed conduction-band background at $T=20$ K and is modeled by the convolution of a Fermi distribution at respective temperature and a Gaussian with a FWHM of the experimental broadening $\Delta E=39$ meV.

of the intense Cu $3d$ band. The Yb $4f^{13}$ peaks sit on-top of a wide In $5sp$ /Yb $5d$ -hybridized conduction band,²⁵ whose intensity can be assumed to be approximately constant up to the onset of the Cu $3d$ band.

The $4f^{13}$ spectra of some scraped surfaces show an additional feature at $E_B \approx 250$ meV with a width below 300 meV (not shown here), which was already reported in Ref. 6. The lack of a spin-orbit partner typical for the Yb $4f^{13}$ states and the sensitivity to surface contaminations seem to indicate that this peak could be of similar nature as the d -like surface state found for Yb metal (111).²⁶ This feature will not be discussed here further because its appearance does not affect the time or temperature dependence of the Yb $4f$ intensities.

B. Intensity of the Yb $4f_{7/2}^{13}$ peak

First, we focus on the feature nearest to the Fermi energy, namely, the (“bulk”) Yb $4f_{7/2}^{13}$ peak, whose intensity is strongly temperature dependent. As a demonstration Fig. 2 shows two normalized spectra of the Yb $4f_{7/2}^{13}$ peak at 20 K (open circles) and 135 K (solid line), respectively. The peak in the 20-K spectrum is approximately twice as intense as in the 135-K spectrum. The inset of Fig. 2 shows high-

resolution data measured at 20 and 150 K with $h\nu=22.4$ eV. The intrinsic Yb $4f_{7/2}^{13}$ linewidth [full width at half maximum (FWHM)] at 20 K amounts to ≈ 50 meV, the position of the maximum is ≈ 44 meV at an experimental resolution of $\Delta E_{\text{RES}}=39$ meV. While raising the temperature to 150 K the photoemission spectra show no indication of an increasing linewidth. The peak maximum shifts slightly (< 10 meV) away from the Fermi energy, a shift that is of the order of magnitude expected from the thermal broadening of the Fermi edge at 150 K.

For the determination of the spectral weight of the Yb $4f_{7/2}^{13}$ line we use a constant non- $4f$ “conduction-band” background, which is cut off by an experimentally broadened Fermi distribution (cf. inset of Fig. 2). Since the spectra show no intensity variation in the “valley” at $E_B \approx 0.4$ eV whereas the intensity of the $4f$ peaks changes substantially, the contribution from a high-energy tail of the Yb $4f_{7/2}^{13}$ peak must be negligible. Therefore the constant non- $4f$ background is normalized to the spectral intensity at $E_B=0.4$ eV. After subtracting this normalized background the $4f$ spectral weight was determined by direct integration over the Yb $4f_{7/2}^{13}$ peak. We note that the background here is an upper limit for the true non- $4f$ spectrum and can thus lead to a possible underestimation of the divalent $4f$ weight and hence to an overestimation of the Yb valence. However, as will be discussed further below, the use of any other realistic background would not affect the conclusions of the following analysis and would even enhance the observed discrepancies between the PES and bulk valences.

Figure 3 displays in detail the variation of the background-corrected integrated Yb $4f_{7/2}^{13}$ intensities: The point labeled 1 was obtained at 20 K measured immediately after crystal cleavage at the same temperature. In a first warming-up sequence (triangles pointing to higher T) up to ≈ 140 K (ending in point 2) the relative Yb $4f_{7/2}^{13}$ intensity decreases continuously to $\approx 50\%$ of its original value. Cooling down again to 20 K (triangles pointing to lower T , ending in point 3) increases the spectral weight again, but the low-temperature intensity is approximately 20% below the initial value of point 1. The Yb $4f^{13}$ spectra of Fig. 2 correspond to point 1, 2, and 3 of Fig. 3. Although the Yb $4f_{5/2}$ line at 1.6 eV overlaps the surface core-level states, Fig. 2 shows also that its intensity behaves analogously to the Yb $4f_{7/2}^{13}$ spectral weight. A more detailed analysis of the Yb $4f_{5/2}^{13}$ intensity after subtraction of a linear background shows that the intensity ratio between the (bulk) $4f$ spin-orbit partners is independent on the temperature and time (see below) and amounts to 1.4 ± 0.1 , near the statistical ratio of 4/3 (8:6). The apparent change of the Yb $4f$ surface contribution in Fig. 2 will be discussed later.

In a further warming-up sequence up to 150 K (point 4 in Fig. 3) and 220 K (point 5) the $4f$ intensity drops down to even 25% of its original value at 20 K. Recooling to 20 K (point 7) the Yb $4f^{13}$ spectral weight clearly increases again, but lies now even further below that of the freshly cleaved surface (1).

From a number of analogous measurements on different samples and under varied conditions it is concluded that this hysteretic loss of $4f$ weight is strongly dependent on the duration of the measurement and the maximum temperature

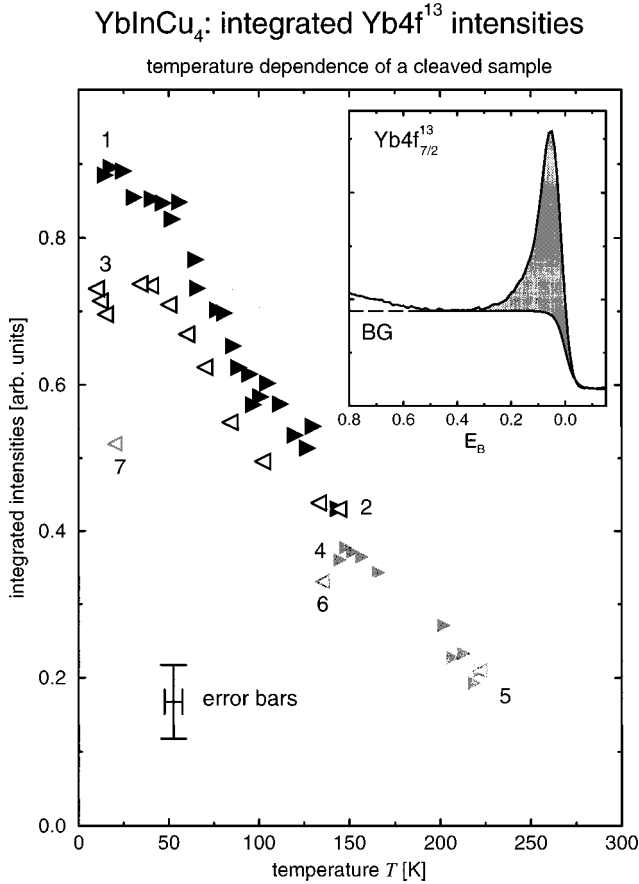


FIG. 3. Yb $4f_{7/2}^{13}$ intensity vs temperature. The intensity is determined from the integrated Yb $4f_{7/2}^{13}$ spectral weight after background subtraction and normalizing to the second-order intensity above the Fermi energy (see inset). Point 1 refers to a measurement at $t=0.5$ h after the cleavage, 2 is the end point of a warming-up sequence at 135 K ($t=4$ h). Point 3 is the end point of a following cooling sequence ($t=5.5$ h). The further labeled points are measured at $t=9$ h (4), 10 h (5), 10.5 h (6), and 11 h (7). The triangles points in the direction of the individual temperature sequence; the error bar gives the systematic error of the determined intensity and temperature.

reached in the heating-cooling cycle. Measurements of the Yb $4f_{7/2}^{13}$ intensities over an extended period of time at fixed temperature confirm that the rate of the intensity loss increases with the temperature; at 300 K the Yb $f_{7/2}^{13}$ weight decreases to about 50% within a few hours, whereas at 20 K the intensity reduction is less than 5% over the same period. From these observations we conclude that the Yb $4f^{13}$ intensity is determined by an intrinsic temperature dependence superimposed by an extrinsic decay with time, which itself is temperature dependent and gives rise to the observed hysteresis.

C. Phenomenological model for the extrinsic intensity loss

In the following we try to describe the time and temperature dependence of the *extrinsic* nonsurface Yb $4f_{7/2}^{13}$ weight loss in a simple phenomenological model. For this purpose we distinguish between two Yb species, one (A) being responsible for the entire initial Yb $4f$ spectrum and therefore

also for the nonsurface $4f_{7/2}^{13}$ intensity at the Fermi level, and another (relaxed) one (B), which contributes, in first order, negligibly to the Yb $4f^{13}$ intensity. The latter assumption is justified if the valence of species B is close to 3+. The outermost divalent Yb ions (species C), responsible for the surface features in the Yb $4f^{13}$ spectra, have no contribution to the nonsurface Yb $4f_{7/2}^{13}$ intensity near E_F and will be neglected in the following.

In this ansatz the Yb $4f^{13}$ weight is caused completely by species A, and the intensity of the Yb $4f_{7/2}^{13}$ peak is thus proportional to its amount N_A . At constant temperature T the reduction $-dN_A$ of atoms of type A (transforming into type B) during a period dt is assumed to be proportional to their total number $N_A(t)$. Therefore, the intensity I_{13} of the nonsurface Yb $4f^{13}$ signal decreases during the time interval Δt by a factor $\exp[-\alpha(T)\Delta t]$. A conceivable way to account for the temperature dependence is by a thermally activated process of the *Arrhenius* type. With an activation energy E_a and the reciprocal time factor β the decay constant can be expressed by $\alpha(T) = \beta \exp(-E_a/k_B T)$. From a linear least-squares fit to the intensity change with time at fixed temperatures T one obtains parameters which can be used to correct for the extrinsic time dependence of the intensities in the heating-cooling cycles. For different samples the resulting parameter β ranges typically from $0.5 \times 10^{-3} \text{ min}^{-1}$ to $3 \times 10^{-3} \text{ min}^{-1}$, the activation energy E_a amounts to a few meV ($\approx 1-5$ meV). This is a surprisingly low activation energy, much smaller than typically encountered in diffusion or adsorption processes. We will return to this point in Sec. IV. If we take the sample history into account, i.e., how long (Δt_i) the surface stayed at certain temperatures T_i , the Arrhenius ansatz now allows one to correct the intensity values of sequentially recorded data for the extrinsic “aging” effect.

As an example we have applied this procedure to the raw data of Fig. 4(a), which show the integrated Yb $4f_{7/2}^{13}$ intensities of a sample that was exposed to several thermal cycles and different surface preparations. Here the spectra have been measured with a photon energy of $h\nu=22.4$ eV with slightly reduced $4f$ cross sections compared to the conduction-band states (see inset of Fig. 2) Fig. 4(b) shows the data after correction with the model above. The resulting curve represents the initial Yb $4f_{7/2}^{13}$ intensities corresponding to a freshly cleaved sample, consisting completely of the aforementioned Yb species type A. The fact that all data, which belong to the same surface preparation method but to quite different stages in the heating-cooling cycles, fall onto a single curve confirms the plausibility of our model on an empirical level. It is also evident that the “intrinsic” Yb $4f_{7/2}^{13}$ weight of the scraped surface lies consistently below that of the cleaved one.

D. Yb valence and its temperature dependence

The Yb $4f$ spectral weight distribution can be used to determine the valence v or the $4f$ hole-occupation number $n_h = v - 2$, of the Yb ions directly from the PES data. Taking the ratio I_{13}/I_{12} of the integrated $4f^{13}$ and $4f^{12}$ intensities yields for the hole-occupation number $n_h = 1/(1 + \frac{13}{14} I_{13}/I_{12})$. Figure 5 displays the valence variation thus obtained for scraped (open symbols) and cleaved (filled sym-

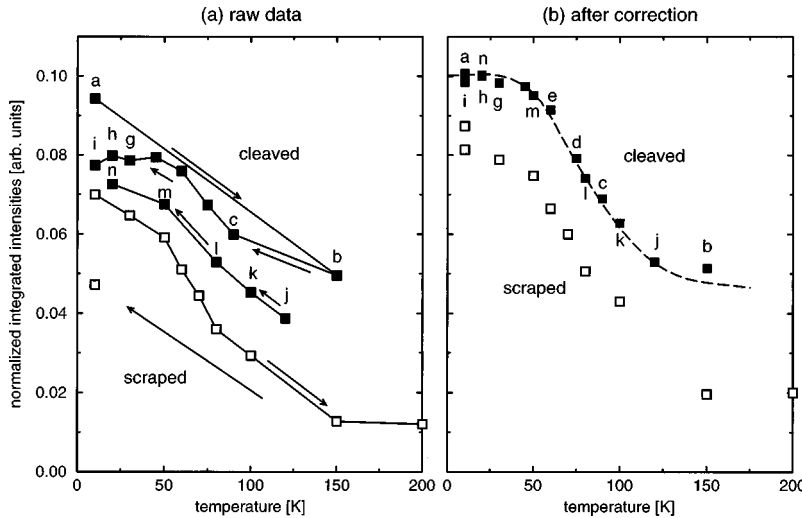


FIG. 4. Integrated Yb $4f_{7/2}^{13}$ intensities vs temperature, (a) raw data, and (b) corrected for the extrinsic intensity loss with time (see text for details). The filled squares (■) refer to a freshly cleaved sample, the open squares (□) to a scraped sample surface. The parameters of the correction for both samples are $E_a = 1.7$ meV and $\beta = 7.4 \times 10^{-4} \text{ min}^{-1}$, determined from the cleaved single-crystalline surface.

bol) single-crystalline samples in the temperature range between 20 and 260 K taking the extrinsic aging effects into account. The maximum error in the spectral weight integration resulting from uncertainties in the background subtraction amounts to $\Delta n_h = \Delta v = 0.05$. Most data points were taken within a short time interval after surface preparation and are thus only marginally affected by the extrinsic effect. Only for a few data points, particularly after exposure to higher temperatures, was it necessary to correct for the aging using the model above.

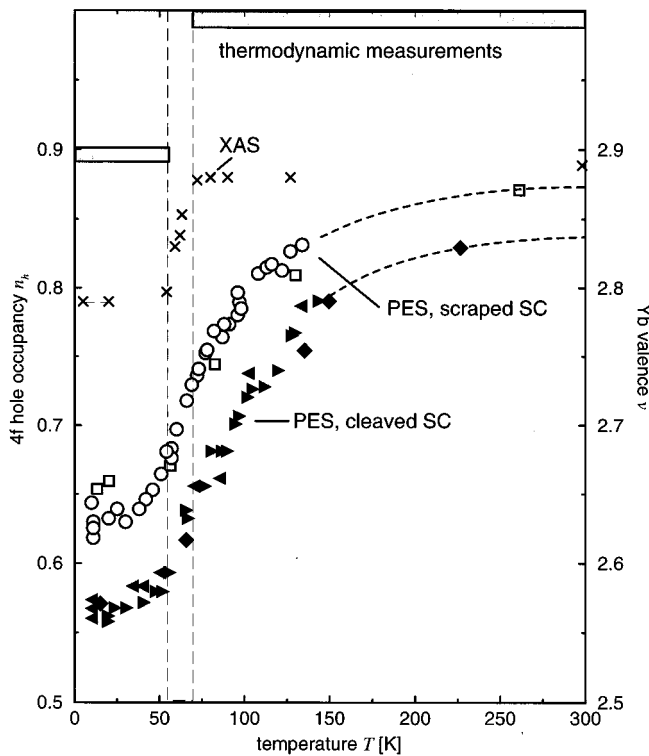


FIG. 5. Yb $4f$ hole occupancy n_h and Yb valence v vs temperature. The filled and the open symbols represent the $n_h(T)$ values resulting from our PES measurements on several freshly cleaved and scraped single crystals (SC), respectively; the dashed lines are only a guide for the eye. The crosses represent the results of XAS measurement of Ref. 1. Thermodynamic measurements (indicated by shaded bars) yield a valence of 3.0+ above, and 2.9+ below the transition temperature.

First we want to concentrate on the results for the cleaved crystals, which exhibit a continuous change from $v = 2.56$ at 20 K to $v = 2.83$ at 230 K. There is no indication of a sudden valence transition, as it was observed, e.g., in the x-ray absorption spectra at the L_{III} edge presented in Ref. 1. In that experiment the valence change was confined to a narrow temperature range of only 10 K around $T_a \approx 63$ K, with the valence changing from 2.79 to 2.88 (crosses in Fig. 5), which is slightly below the values estimated from susceptibility and lattice constant measurements (indicated by shaded bars in Fig. 5). In contrast, the valence change extracted from the PES data extends over a broad temperature range of more than 60 K, with the hole-occupation number $n_h(T)$ always remaining significantly below the results of the bulk-sensitive experiments, a result that is also found for other intermediate valent Yb compounds.¹⁶ The different behavior of scraped and cleaved surfaces seen in Figs. 4 and 5 is discussed in the next section.

IV. DISCUSSION

The experimental results raise two questions: (a) What mechanism leads to the extrinsic time-dependent reduction of the Yb $4f^{13}$ final-state intensities? and (b) why does the initial photoemission valence deviate from other, bulk sensitive measurements, both in the number and its T dependence? Given the characteristically small photoemission sampling depth of several atomic layers it seems obvious to attribute these discrepancies to surface-related effects. Therefore we shall discuss surface quality and preparation in more detail.

First we focus on the effect of the surface preparation method on the PES data. Cleavage of single crystals has turned out to be the most reliable technique, in the sense that it leads to reproducible and high Yb $4f^{13}$ intensities. In Ref. 13 it has been shown that there are significant differences between the Yb $4f$ spectra of polycrystalline and single-crystalline material. A “polycrystalline” surface can be produced by *in situ* scraping of a single crystal with a diamond or ceramic file. We found indeed that scraped surfaces never produce the same initially high $4f^{13}$ intensity that was obtained from a cleaved YbInCu₄ crystal, even though the application of the file seemed to result in coarse-grained (i.e.,

consistent of a relatively small number of randomly oriented crystal faces) surfaces. The divalent $4f$ weight is typically 20% lower than on freshly cleaved single-crystal surfaces. Interestingly, the *relative* temperature variation of the Yb $4f^{13}$ intensity remains unchanged: between 20 and 150 K the Yb $4f^{13}$ lines of cleaved and scraped single crystals lose approximately half of their spectral weight [cf. Fig. 4(b)]. The analysis of the I_{13}/I_{12} intensity ratio from spectra of several freshly *in situ* scraped surfaces (open symbols in Fig. 5) leads to the surprising result that in the entire investigated temperature range the valence is slightly *higher* (i.e., closer to the bulk) than the values obtained from single crystals, although it still remains below that obtained by XAS.

With respect to the observed time dependence of the spectra we note that the surfaces of rare-earth compounds are known to be extremely sensitive to oxidation and that contamination by the residual gas in the UHV degrades the surfaces rapidly with time. XPS core-level and valence-band measurements on the YbInCu₄ single crystals performed in our home laboratory²⁷ show that the surfaces indeed oxidize with time, leading to a change of the formal valence towards $3+$, i.e., a loss of Yb $4f^{13}$ intensity. On the other hand, in the highly surface-sensitive PES experiments at $h\nu = 43$ eV we found no indication for the presence of oxygen states in the VB region ($O\ 2s$, $O\ 2p$) before the extrinsic decay of the Yb $4f^{13}$ weight was already noticeably advanced. Figure 6 shows a spectrum of a freshly cleaved sample in comparison to spectra taken of two different samples more than 24 h after the surface preparation, which show pronounced oxidation effects in the $4f^{12}$ range. As the $4f^{12}$ part of the spectrum is most susceptible to oxygen contamination we have used it as a probe for surface quality. We have considered only those spectra as representative of a clean sample, in which the $4f^{12}$ spectrum is clearly distinguishable from a smooth background and shows the sharp $4f^{12}$ multiplet structure expected from atomic theory²² (see inset of Fig. 6). Under the good vacuum conditions during our experiments the surface remained oxygen-free (in the sense mentioned above) for at least 12 h after preparation, with only spectra from clean samples entering the analysis. Therefore we are led to conclude that the observed *initial* decay of the $4f^{13}$ intensity is not caused by mere surface contamination but must be related to a different process.

Before proceeding with the behavior of the nonsurface Yb $4f^{13}$ intensity we note that also the $4f$ contribution caused by the divalent surface atoms exhibits noticeable changes with time and temperature. This can be seen, e.g., in the spectra of Fig. 2 where the surface contributions at $E_B \approx 1.1$ eV shifts to lower binding energies between 20 K (spectrum labeled by 1) and 135 K (2). Recooling to 20 K (3) demonstrates that the shift is irreversible. Detailed PES studies of the pure Yb (111) metal surface have shown that the broad Yb $4f^{13}$ surface spectrum is actually a superposition of several peaks, each of which corresponds to a different coordination of the Yb ion and thus displays its own specific surface core-level shift.²³ We attribute the shift to lower binding energies observed in the data to a rearrangement of the topmost Yb ions, which seek to increase their local coordination. Due to an increase of the atomic mobility the process becomes enhanced as the temperature is raised, accelerating the change of the surface-related $4f$ photoemission weight distribution.

YbInCu₄: oxidation and Yb $4f^{13}$ states $h\nu = 43$ eV, $T = 20$ K

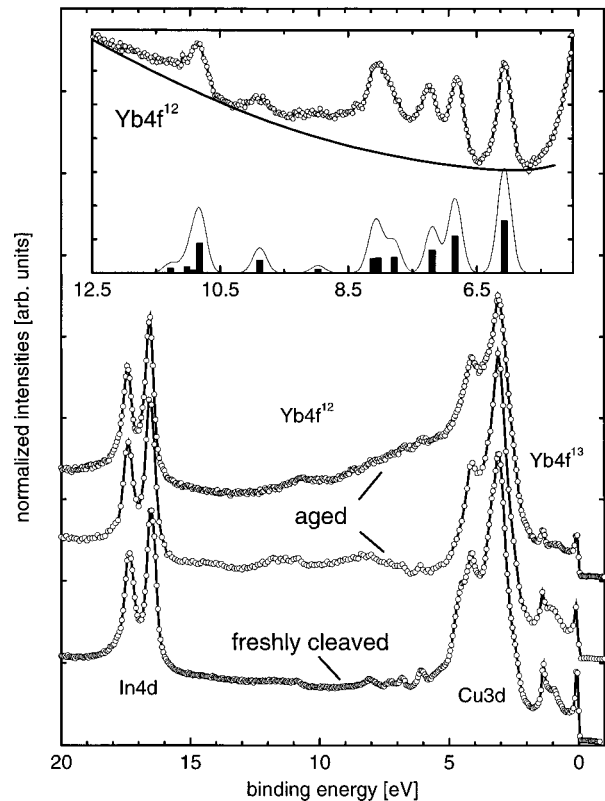


FIG. 6. VB spectra of YbInCu₄ surfaces with different surface qualities. The spectrum at the bottom is taken from a freshly scraped sample, the other spectra are taken from surfaces that have been exposed for more than 24 h. The Yb $4f^{12}$ range of the aged spectra shows considerable contributions from oxidation effects, apparent by different multiplet features and an increased $O\ 2p$ intensity in the energy range from 3 to 7 eV. The inset gives a comparison of the Yb $4f^{12}$ multiplet from a freshly scraped single crystal with the calculated multiplet from Ref. 22 (stretched by a factor of 1.1 and convoluted by a Gaussian with a FWHM of 250 meV). The thick line represents an arbitrary smooth background as used for the determination of the Yb $4f^{12}$ intensities.

However, we wish to point out that the irreversible change of the surface spectra is *not* directly correlated with the behavior of the Yb $4f_{7/2}^{13}$ peak near the Fermi energy, as can be inferred, e.g., from the comparison of spectra (1) and (3) in Fig. 2.

Returning to the extrinsic time-dependent decay of the Yb $4f^{13}$ bulk peak, a first hint to its microscopic origin is possibly contained in our Arrhenius model analysis. As discussed above, the application of the model yields a characteristic energy E_a of only several meV, which in view of the empirical success of the approach seems to rule out diffusion or chemical reaction processes as origin for the spectral changes. Those cases involve activation energies of order of 0.1–1 eV,⁷ orders of magnitude larger than found here. Rather the E_a obtained in the analysis is comparable to the magnitude of energy-per-atom differences, when different structural configurations of a solid or a surface are compared.^{28,29} This suggests that structural relaxation at or near the surface could be a possible explanation for the ini-

tial loss in Yb $4f^{13}$ weight. Since the outermost divalent Yb atoms (species C) do not contribute to the considered Yb $4f_{7/2}^{13}$ intensity, the Yb species type A responsible for the decaying Yb $4f^{13}$ peak at the Fermi level must be found in the subsurface layers. For the following discussion it is hence useful to distinguish between (i) the surface layer consisting of the topmost atoms, responsible for the Yb $4f$ surface feature at 1.1 eV, (ii) the undistorted cubic bulk material without any influence from the surface, and (iii) an intermediate subsurface zone, which may be distorted in comparison to the bulk, possibly due to a multilayer relaxation with an extension over a few lattice constants in the same order of magnitude with the PES probing depth.^{30–32} The existence of such a subsurface region has been raised by Lawrence *et al.*¹⁶ as one possible explanation for the deviating results of XAS and PES regarding the Yb valence of several intermediate-valent Yb compounds.

In the following we try to develop an explanation for the observed numbers and time dependence of the photoemission Yb valence. With no further structural information at hand this is of course somewhat speculative, but as we will show it is possible to find a plausible scenario that provides a consistent description of the photoemission results. In the most simple picture the crystal would immediately after cleavage keep its bulk structure up to the terminating surface. For the surface and near-surface atom layers this configuration does generally not correspond to a thermodynamic equilibrium. Therefore, they will subsequently tend to relax towards a structure that minimizes the total energy (“*distortive*” relaxation) and would result in changes of the electronic structure. However, this behavior does not seem to be consistent with our PES results, because it would drive the properties of the near-surface region *away* from those of the bulk. In contrast, the Yb valence derived from the Yb $4f$ intensity ratio initially starts out from a relatively low value and then starts to change *towards* the value obtained by bulk-sensitive methods.

The apparent failure of this picture leads us to consider a different scenario. Upon creation of the surface the changed environment of the outermost Yb atoms leaves them in a purely divalent state. Since it is known that the ionic radius of Yb^{2+} is about 10% larger than the radius of the trivalent ytterbium³³ the atomic arrangement of the top layer will certainly be distorted (i.e., mainly be expanded) relative to the bulk where the Yb valence is close to trivalence.³⁴ Consequently there must be a distorted subsurface region that buffers the misfit between surface and bulk. If the main aspect of the distortion is indeed an expansion of the lattice (“*negative pressure*”) it would explain the decreased Yb valence (compared to the bulk) observed immediately after cleavage, because experiments on the pressure dependence^{35,36} and on suitably doped YbInCu_4 (Refs. 1 and 18) confirm an increasing stabilization of the divalence with decreasing lattice pressure. Again, this configuration right after cleavage does not necessarily correspond to an energy minimum. This can already be inferred from the time dependence of the Yb $4f$ surface contribution, which signals a rearrangement of the topmost Yb^{2+} ions. Generally, we expect that the entire near-surface region will relax in such a way as to minimize the elastic strain between surface and bulk (“*restoring*” relaxation), i.e., it will tend to the original bulk structure,

though of course this will not be completely possible due to the presence of the terminating surface. As a consequence the initial Yb $4f_{7/2}^{13}$ weight near the Fermi energy will decrease with time, i.e., the valence will tend towards the bulk value. Since the photoelectron mean free path in the solid is only 5–10 Å at kinetic energies near 40 eV, the emission from the subsurface zone is the major contribution to the nonsurface spectral weight. This implies that the $4f^{13}$ weight that we so far have referred to as “*bulk peaks*” actually originates mainly in the subsurface zone.

Unfortunately, the additional surface oxidation on aged surfaces made it impossible to study a relaxed but clean phase in more detail. However, preliminary high-resolution measurements on single-crystalline YbInCu_4 surfaces,³⁷ which have been exposed to the UHV for more than two weeks at a constant temperature of 20 K, give a first indication that the extrinsic time-dependent decrease of the $4f^{13}$ intensity saturates at about a fourth of its initial value. The smooth intrinsic temperature dependence of the $4f^{13}$ spectral weight can still be seen even for this severely aged and contaminated surface. Further insight into a possible surface relaxation could be achieved by temperature and time dependent LEED measurements. This, however, requires well-defined single-crystalline surfaces that are homogeneous and flat over a larger area than the ones obtained here.

It was already mentioned that besides its (initial) number, also the temperature dependence of the Yb valence measured by PES differs distinctly from that in the bulk, which can be explained in mainly two ways. Let us first assume that the valence increase towards higher temperature is still related to the first-order phase transition in the volume. From measurements of the electrical resistivity and the magnetic susceptibility it is known that doping or deviations from the exact integer stoichiometry can lead to a broadening of the transition and/or a change of the transition temperature.^{1,38,18,19} It is conceivable that surface inhomogeneities, both laterally and through the subsurface region, could produce a similar effect. In this case the observed (intrinsic) temperature dependence in Fig. 5 would represent an averaged valence transition over a distribution of near-surface regions with varying thermodynamic properties.

The second explanation is based on the possibility that the temperature dependence of the Yb $4f^{13}$ intensity is not (or not exclusively) related to the bulk phase transition unique for YbInCu_4 but is of the same nature as the temperature dependence of the divalent $4f$ intensities observed in other Yb compounds, e.g., YbAl_3 (Refs. 8 and 39) and YbAgCu_4 .^{9,10,40} In a temperature range from approximately 20 K to more than 250 K these compounds show a continuous decrease of their divalent spectral weight to less than 50%. Two competing origins for the intensity decrease have been discussed throughout the literature:^{8,10–14} (i) a thermal singlet-triplet excitation described by the SIAM within the noncrossing approximation^{41,42} (NCA), which leads to a temperature dependence of the Yb valence and thus to a transfer of spectral weight from the divalent to the trivalent contribution, (ii) conventional effects known from core-level spectroscopy, which are mainly due to electron-phonon coupling. However, as our spectra show no phonon-related broadening of the $4f$ linewidth in the studied temperature range, which lies well below the Debye temperature of about 280 K,⁴³

electron-phonon coupling is a less likely source for the temperature dependence of the divalent spectral weight in YbInCu₄.

It is interesting to note that the sharp valence phase transition in bulk YbInCu₄ can be smeared out or even suppressed by substitution of the In atoms by Ag,^{4,17,19} with the resulting temperature dependence of the (bulk) valence in YbIn_{1-x}Ag_xCu₄ becoming strongly reminiscent of the behavior of the PES valence in pure YbInCu₄. This indicates that the subsurface zone probed by PES is similarly distorted and/or disordered than the volume material in YbIn_{1-x}Ag_xCu₄. The thermodynamic properties of YbIn_{1-x}Ag_xCu₄ have recently been discussed in the framework of the SIAM.^{4,17} A detailed analysis of our PES data in this sense would go beyond the scope of this paper and seems premature as long as the structural nature of the surface/subsurface remains unclear.

V. CONCLUSIONS

High-resolution photoemission measurements on YbInCu₄ give evidence for pronounced surface effects on the Yb 4*f* spectra. The spectral weight of the Yb 4*f*_{7/2}¹³ peak at the Fermi level, being a fingerprint for the mixed-valent character of the Yb ions, is found to display a strong intrinsic temperature dependence caused by a valence change of the sampled Yb ions. This temperature dependence is superimposed by an irreversible decay of the Yb 4*f*¹³ intensity with time. The extrinsic intensity loss seems to follow an activated behavior with a characteristic energy of a few meV, possibly related to a structural relaxation of the subsurface region after initial distortion by crystal cleavage. The intrinsic valence, corresponding to a freshly cleaved surface and directly derived from the ratio of the 4*f*¹² and 4*f*¹³ spectral weights, varies continuously from $\nu = 2.56$ to 2.85 between 20 and 220 K, remaining systematically below the values

obtained by bulk-sensitive methods and showing no indication of a sharp valence transition as observed in the volume material.

This can be consistently explained by the existence of a subsurface region with individual thermodynamic and spectroscopic properties, which mediates the lattice strain between the large divalent outermost Yb ions and the smaller nearly trivalent ions deep inside the bulk. One may feel inclined to infer that this conclusion is not restricted to the particular case of YbInCu₄ studied here, but could also be of relevance for other Yb compounds, where divalent Yb surface atoms exist in spite of an unstable intermediate-valence close to Yb³⁺ in the volume and where discrepancies between photoemission results and more bulk-sensitive data have been reported.

However, it is important to realize that, if the SIAM is indeed the correct model to describe the electronic structure, one cannot expect the subsurface region to be characterized by the same model parameters (e.g., the Kondo temperature⁴⁴) as the bulk. This may add a new aspect to the highly controversial discussion on the relevance of the Kondo picture for Yb PES data, for which we refer to Refs. 8,11–14 and the review article by Malterre *et al.*¹⁰

ACKNOWLEDGMENTS

We like to thank C. Kim, C.-H. Park, A. Matsuura, and Z.-X. Shen (Stanford) for their support during the synchrotron radiation measurements and especially G. Reichardt (Berlin) for his help at the undulator beam-line at BESSY. We also thank C. Geibel (TH Darmstadt) for fruitful discussions about mixed-valent Yb systems. This work was funded by the Bundesministerium für Forschung und Technologie (Project No. 13N6602), the Deutsche Forschungsgemeinschaft (CI 124/2-1), and the U.S. DOE (Grant No. DE-FG02-90ER45416).

¹I. Felner, I. Nowik, D. Vaknin, U. Potzel, J. Moser, G. M. Kalvius, G. Wortmann, G. Schmiester, G. Hilscher, E. Gratz, C. Schmitzer, N. Pillmayr, K. G. Prasad, H. de Waard, and H. Pinto, *Phys. Rev. B* **35**, 6956 (1987).

²B. Kindler, D. Finsterbusch, R. Graf, F. Ritter, W. Assmus, and B. Lüthi, *Phys. Rev. B* **50**, 704 (1994).

³I. Felner and I. Nowik, *Phys. Rev. B* **33**, 617 (1986).

⁴J. L. Sarrao, C. D. Immer, C. L. Benton, Z. Fisk, J. M. Lawrence, D. Mandrus, and J. D. Thompson, *Phys. Rev. B* **54**, 12 207 (1996).

⁵S. Ogawa, S. Suga, M. Taniguchi, M. Fujisawa, A. Fujimori, T. Shimizu, H. Yasuoka, and K. Yoshimura, *Solid State Commun.* **67**, 1093 (1988).

⁶M. Okusawa, E. Weschke, R. Meier, G. Kaindl, T. Ishii, N. Sato, and T. Komatsubara, *J. Electron Spectrosc. Relat. Phenom.* **78**, 139 (1996).

⁷*Handbook on the Physics and Chemistry of Rare Earths*, edited by K. A. Gschneidner, Jr. and L. R. Eyring (North-Holland, Amsterdam, 1982).

⁸L. H. Tjeng, S.-J. Oh, E.-J. Cho, H.-J. Lin, C. T. Chen, G.-H. Gweon, J.-H. Park, J. W. Allen, T. Suzuki, M. S. Makić, and

D. L. Cox, *Phys. Rev. Lett.* **71**, 1419 (1993).

⁹P. Weibel, M. Grioni, D. Malterre, B. Dardel, Y. Baer, and M. J. Besnus, *Z. Phys. B* **91**, 337 (1993).

¹⁰D. Malterre, M. Grioni, and Y. Baer, *Adv. Phys.* **45**, 299 (1996).

¹¹J. J. Joyce, A. J. Arko, A. B. Andrews, and R. I. R. Blyth, *Phys. Rev. Lett.* **72**, 1774 (1994).

¹²L. H. Tjeng, S.-J. Oh, C. T. Chen, J. W. Allen, and D. L. Cox, *Phys. Rev. Lett.* **72**, 1775 (1994).

¹³R. I. R. Blyth, J. J. Joyce, A. J. Arko, P. C. Canfield, A. B. Andrews, Z. Fisk, J. D. Thompson, R. J. Bartlett, P. Riseborough, J. Tang, and J. M. Lawrence, *Phys. Rev. B* **48**, 9497 (1993).

¹⁴J. J. Joyce, A. B. Andrews, A. J. Arko, R. J. Bartlett, R. I. R. Blyth, C. G. Olson, P. J. Benning, P. C. Canfield, and D. M. Poirier, *Phys. Rev. B* **54**, 17 515 (1996).

¹⁵A. B. Andrews, J. J. Joyce, A. J. Arko, Z. Fisk, and P. S. Riseborough, *Phys. Rev. B* **53**, 3317 (1996).

¹⁶J. M. Lawrence, G. H. Kwei, P. C. Canfield, J. G. DeWitt, and A. C. Lawson, *Phys. Rev. B* **49**, 1627 (1994).

¹⁷A. L. Cornelius, J. M. Lawrence, J. L. Sarrao, Z. Fisk, M. F. Hundley, G. H. Kwei, J. D. Thompson, C. H. Booth, and F.

- Bridges, Phys. Rev. B **56**, 7993 (1997).
- ¹⁸C. D. Immer, J. L. Sarrao, Z. Fisk, A. Lacerda, C. Mielke, and J. D. Thompson, Phys. Rev. B **56**, 71 (1997).
- ¹⁹J. L. Sarrao, C. L. Benton, Z. Fisk, J. M. Lawrence, D. Mandrus, and J. D. Thompson, Physica B **223&224**, 366 (1996).
- ²⁰I. Aviani, M. Miljak, V. Zlatić, D. Finsterbusch, W. Assmus, and B. Lüthi, Physica B **230–232**, 275 (1997).
- ²¹B. Kindler, Ph.D. thesis, Frankfurt am Main, 1994.
- ²²F. Gerken, J. Phys. F **13**, 703 (1983).
- ²³W.-D. Schneider, C. Laubschat, and B. Reihl, Phys. Rev. B **27**, 6538 (1983).
- ²⁴C. Laubschat, G. Kaindl, W.-D. Schneider, B. Reihl, and N. Mårtensson, Phys. Rev. B **33**, 6675 (1986).
- ²⁵K. Takegahara and T. Kasuya, J. Phys. Soc. Jpn. **59**, 3299 (1990).
- ²⁶M. Bodenbach, A. Höhr, C. Laubschat, and G. Kaindl, Phys. Rev. B **50**, 14 446 (1994).
- ²⁷S. Schmidt, Master's thesis, Universität des Saarlandes, 1998.
- ²⁸Z. Szotek, W. M. Temmerman, and H. Winter, Phys. Rev. Lett. **72**, 1244 (1994).
- ²⁹A. Svane, Phys. Rev. Lett. **72**, 1248 (1994).
- ³⁰D. L. Adams and C. S. Sørensen, Surf. Sci. **166**, 495 (1986).
- ³¹L. I. Johansson, H. I. P. Johansson, J. N. Andersen, E. Lundgren, and R. Nyholm, Phys. Rev. Lett. **71**, 2453 (1993).
- ³²M. Aldén, H. L. Skriver, and B. Johansson, Phys. Rev. Lett. **71**, 2449 (1993).
- ³³J. M. Lawrence, P. S. Riseborough, and R. D. Parks, Rep. Prog. Phys. **44**, 1 (1981).
- ³⁴A. Stenborg, J. N. Andersen, O. Björneholm, A. Nilsson, and N. Mårtensson, Phys. Rev. Lett. **63**, 187 (1989).
- ³⁵I. Nowik, I. Felner, J. Voiron, J. Beille, A. Najib, E. du Tremolet de Lacheisserie, and G. Gratz, Phys. Rev. B **37**, 5633 (1988).
- ³⁶J. M. De Teresa, Z. Arnold, A. del Moral, M. R. Ibarra, J. Kamarád, D. T. Adroja, and B. Rainford, Solid State Commun. **99**, 911 (1996).
- ³⁷F. Reinert, G. Nicolay, R. Claessen, S. Hüfner, and W. Assmus (unpublished).
- ³⁸J. M. Lawrence, G. H. Kwei, J. L. Sarrao, Z. Fisk, D. Mandrus, and J. D. Thompson, Phys. Rev. B **54**, 6011 (1996).
- ³⁹S.-J. Oh, S. Suga, A. Kakizaki, M. Taniguchi, T. Ishii, J.-S. Kang, J. W. Allen, O. Gunnarsson, N. E. Christensen, A. Fujimori, T. Suzuki, T. Kasuya, T. Miyahara, H. Kato, K. Schönhammer, M. S. Torikachvili, and M. B. Maple, Phys. Rev. B **37**, 2861 (1988).
- ⁴⁰D. Malterre, M. Grioni, P. Weibel, B. Dardel, and Y. Baer, Physica B **199&200**, 76 (1994).
- ⁴¹N. E. Bickers, D. L. Cox, and J. W. Wilkins, Phys. Rev. B **36**, 2036 (1987).
- ⁴²Y. Kuramoto and H. Kojima, Z. Phys. B **57**, 95 (1984).
- ⁴³E. V. Sampathkumaran, N. Nambudripad, S. K. Dhar, R. Vijayaraghavan, and R. Kuentzler, Phys. Rev. B **35**, 2035 (1987).
- ⁴⁴M. Garnier, K. Breuer, D. Purdie, M. Hengsberger, Y. Baer, and B. Delley, Phys. Rev. Lett. **78**, 4127 (1997).